NASA TECHNICAL NOTE

NASA TN D-2805

NASA TN D-2805

ANALYTICAL LIFETIME STUDIES OF A CLOSE-LUNAR SATELLITE

by William R. Wells

Langley Research Center
Langley Station, Hampton, Va.

NATIONAL AERONAUTICS AND SPACE ADMINISTRATION • WASHINGTON, D. C. • MAY 1965

NASA TN D-2805

ANALYTICAL LIFETIME STUDIES OF A CLOSE-LUNAR SATELLITE

By William R. Wells

Langley Research Center
Langley Station, Hampton, Va.

NATIONAL AERONAUTICS AND SPACE ADMINISTRATION

For sale by the Clearinghouse for Federal Scientific and Technical Information
Springfield, Virginia 22151 – Price $2.00

ANALYTICAL LIFETIME STUDIES OF A CLOSE-LUNAR SATELLITE

By William R. Wells
Langley Research Center

SUMMARY

An analytical study has been made to determine the influence of the third zonal harmonic of the moon on the lifetime of close-lunar satellites. The orbits considered are applicable to a close-lunar photographic mission and for a mission to determine the magnitude of the coefficient of the third zonal harmonic of the moon J_{30}. The lunar model used in the analysis has oblateness, equatorial ellipticity, and a nonsymmetric distribution of mass in the northern and southern hemispheres; that is, the gravitational potential function includes terms involving the coefficients of the zonal and sectorial harmonics J_{20}, J_{22}, and J_{30} in addition to the point-mass contribution.

Target-site selection for a photographic mission is considered for orbits with initial arguments of pericentron corresponding to optimum lifetimes based on a given magnitude of J_{30} (independent of its sign). With this constraint imposed on the initial argument of pericentron, the effect of inclination on the target sites and rate of change of pericentron altitude is considered. This phase of the analysis is considered by using several values for the magnitude of J_{30}. (Pericentron is defined as the point in the orbit of one body about another at which the least separation of the two bodies occurs.)

INTRODUCTION

In order to design proper orbital elements for lunar missions having close-approach orbits, it is necessary to obtain an estimation of possible maximum perturbations on the satellite. The major perturbations arise from the disturbing influence of the earth and sun and from the higher order harmonics of the lunar gravitational potential function. A principal perturbation on a close-lunar satellite is due to the mass anomalies which are expressed mathematically in the gravitational potential function in the form of the coefficients of the higher order harmonics such as J_{20}, J_{22}, and J_{30}. The harmonic with coefficient J_{30} causes a first-order change in the eccentricity of the orbit and consequently in its pericentron altitude. The harmonics with coefficients J_{20} and J_{22} cause no change and second-order changes, respectively, in the eccentricity, and for this reason only the effect of the third zonal harmonic on the satellite lifetime will be considered.

Until a lunar satellite is established there will be no data available for making analytical calculations of the J_{30} coefficient for the moon. The situation is analogous to that for the earth, for which the pear-shape effect was discovered after analysis of tracking data from the first earth satellites. The best that can be done at present is to make estimates of the J_{30} value for the moon based on knowledge of corresponding values for the earth. These approximations may turn out to be rather gross but they do provide a starting point.

It has been suggested in reference 1 that estimates of the coefficients of the higher harmonics of the lunar gravitational potential can be based on the assumption that the moon and earth can support equal stresses. For a smaller and less massive body, a given stress implies greater gravitational anomalies than for a larger body. A simple dimensional analysis on the stress and the equal stress assumption indicate that corresponding coefficients of the moon can be some 36 times those for the earth. The maximum value of J_{30} for the earth has been estimated from studies of earth-satellite tracking data to be about -2.6×10^{-6}. This means that the magnitude of J_{30} for the moon may be as large as 9.3×10^{-5} if the equal stress assumption is true.

In the absence of a J_{30} term, close satellites of the moon would have essentially an indefinite lifetime (ignoring solar and earth perturbations). The presence of a J_{30} term causes long periodic perturbations (period of about a year) which will limit the lifetime of these satellites; the amount of limitation depends on the initial conditions under which the orbit is established. Since long lifetimes are generally desirable for most missions, it is natural to look for situations for which long lifetimes are obtained even though the magnitude and sign of J_{30} are not known. At the same time, since an analysis to determine the lunar gravitational field is part of any mission, the orbits should be designed so that the value of J_{30} can be estimated from tracking data. It will be shown in this analysis that these two features can be obtained simultaneously by a proper choice of the initial value of the argument of pericentron which is the essential parameter in the analysis.

SYMBOLS

a semimajor axis of Keplerian orbit, km

$\dot{E}$ time rate of change of a general element

e eccentricity of a Keplerian orbit

$$f = \frac{J_{30}R_m}{2J_{20}a(1 - e^2)} \frac{\sin^2 i - e^2\cos^2 i}{e \sin i}$$

G	universal gravitational constant
i	orbit inclination referred to lunar equator, deg
J_{20}	coefficient of second zonal harmonic of lunar gravitational potential function, taken as 2.073×10^{-4}
J_{22}	coefficient of second sectorial harmonic of lunar gravitational potential function, taken as -2.03×10^{-5}
J_{30}	coefficient of third zonal harmonic of lunar gravitational potential function
J_{nm}, K_{nm}	general coefficients in lunar gravitational potential function
M	mean anomaly, deg
n	mean motion of lunar satellite in Keplerian orbit, rad/day
n_1	mean motion of moon about its polar axis, 0.23 rad/day
P_{nm}	associated Legendre function, $P_{nm}(\sin \phi)$
$\vec{r}$	position vector from center of moon to satellite, km
r	distance from center of moon to satellite, km
r_p	distance from center of moon to satellite at pericentron, km
Δr_p	increment of change in pericentron distance, km
R	disturbing function due to mass anomalies, km^2/day^2
R_m	mean radius of moon, 1738.1 km
t	time, days
T	satellite lifetime, days
U	lunar gravitational potential function, km^2/day^2
v	true anomaly, deg
x,y,z	Cartesian coordinates of satellite referred to moon-centered axis system, directions fixed in space, km
x',y',z'	Cartesian coordinates of an element of mass, referred to moon-centered axis system, km
$X_o^{n,m}$	Hansen coefficient
γ	vernal equinox
Δ	operation denoting incremental change

δ Kronecker delta function

θ longitude of satellite measured in equatorial plane of moon from the mean earth-moon line, positive eastward, deg

μ product of gravitational constant and mass of moon, 3.6601×10^{13}, km^3/day^2

σ longitude of sun relative to mean earth-moon line, deg

ϕ latitude of satellite measured from the lunar equator, positive northward, deg

ω argument of pericentron, deg

$\dot{\omega}_s = \frac{3nJ_{20}R_m^2}{a^2(1 - e^2)^2}\left(1 - \frac{5}{4}\sin^2 i\right)$, secular rate of argument of pericentron, rad/day

$(\omega_o)_m$ initial argument of pericentron corresponding to optimum lifetime, deg

Ω longitude, from vernal equinox, of ascending node of Keplerian orbit, deg

Ω' longitude of ascending node measured from the mean earth-moon line positive eastward, deg

Subscripts:

E earth

o initial value

1 short-period terms

2 long-period terms (half the rotational period of the moon about its polar axis)

3 long-period terms (period of the line of apsides of the lunar orbit)

4 secular terms

A dot over a symbol represents differentiation with respect to time.

A bar over a quantity in parentheses denotes the mean value of that quantity.

GENERAL CONSIDERATIONS

Lunar Model and First-Order Perturbation Analysis

The mutual attraction between a body with finite size and a body considered as a point mass can be studied by analyzing the motion of the point

mass relative to the finite body. This motion is expressed mathematically as

$$\ddot{\vec{r}}(x,y,z) = \vec{F}(x,y,z) \tag{1}$$

where $\vec{r}$ is the position vector of the satellite or point mass relative to the mass center of the moon or finite mass and $\vec{F}$ is the mutual force of attraction, per unit of satellite mass, between these two bodies.

The force field $\vec{F}$ is conservative since it is due to gravitational attraction only and, as such, can be represented as the gradient of a scalar U called the gravitational potential function, that is,

$$\ddot{\vec{r}} = \nabla U \tag{2}$$

or

$$\ddot{\vec{r}} = \nabla U \tag{3}$$

The gravitational potential function per unit satellite mass for each element of the attracting body is directly proportional to the element of mass and the universal gravitational constant and inversely proportional to the distance separating this element of mass and the satellite. The potential function per unit of satellite mass for the totality of elements of the finite body is then expressed as

$$U = G \iiint_M \frac{dM(x',y',z')}{\left[(x - x')^2 + (y - y')^2 + (z - z')^2\right]^{1/2}} \tag{4}$$

where M in equation (4) is the mass of the attracting body.

The potential function can be expressed in terms of the latitude and longitude of the satellite relative to coordinates on the surface of the moon and the distance of the satellite from the center of mass of the moon. This expression can be made by recognizing that the gravitational potential satisfies Laplace's equation for points exterior to the moon's surface and by solving this equation for U in terms of spherical harmonics (ref. 2). Laplace's equation is

$$\nabla^2 U = 0 \tag{5}$$

The solution of equation (5) in terms of the notation of the present paper is

$$U(r,\theta,\phi) = \frac{\mu}{r}\left[1 - \sum_{n=1}^{\infty}\sum_{m=0}^{n}\left(\frac{R_m}{r}\right)^n (J_{nm}\cos m\theta + K_{nm}\sin m\theta)P_{nm}(\sin\phi)\right] \tag{6}$$

The solution of Laplace's equation as given by equation (6) is given in references 2 and 3. In the present analysis it is assumed that the potential function given by equation (6) can be approximated by the terms having coefficients J_{20}, J_{22}, and J_{30}. These harmonics account for whatever oblateness, equatorial ellipticity, and pear-shape is present. This assumption gives the following expression for the potential function:

$$U(r,\theta,\phi) = \frac{\mu}{r}\left[1 + \frac{R_m^2}{2r^2} J_{20}\left(1 - 3\sin^2\phi\right) - \frac{3R_m^2}{r^2} J_{22}\cos^2\phi\cos 2\theta - \frac{R_m^3}{2r^3} J_{30}\sin\phi\left(5\sin^2\phi - 3\right)\right] \tag{7}$$

The first term on the right-hand side of equation (7) is the potential due to a point mass; the second term accounts for the oblateness of the moon; the third term accounts for the ellipticity of the equator, and the fourth term accounts for a nonsymmetric distribution of mass in the northern and southern hemispheres (pear-shape effect).

The first-order perturbations of the elements (excluding mean anomaly M) of the close-lunar orbit on the values obtained for a point mass are developed in appendix A and are given here for reference and include both long-period effects and the secular effects:

$$\Delta a = 0 \tag{8a}$$

$$\Delta e = -\frac{J_{30}R_m}{2aJ_{20}}\sin i(\sin\omega - \sin\omega_o) \tag{8b}$$

$$\Delta\omega = \frac{3nJ_{20}R_m^2}{a^2(1-e^2)^2}\left(1 - \frac{5}{4}\sin^2 i\right)t + \frac{3nJ_{22}R_m^2}{2n_1a^2(1-e^2)^2}\left(1 - \frac{5}{2}\sin^2 i\right)\left(\sin 2\Omega' - \sin 2\Omega_o'\right) - \frac{J_{30}R_m}{2aJ_{20}(1-e^2)}\frac{\sin^2 i - e^2\cos^2 i}{e\sin i}(\cos\omega - \cos\omega_o) \tag{8c}$$

$$\Delta i = \frac{3nJ_{22}R_m^2\sin i}{2a^2n_1(1-e^2)^2}\left(\cos 2\Omega' - \cos 2\Omega_o'\right) + \frac{J_{30}R_m e\cos i}{2J_{20}a(1-e^2)}(\sin\omega - \sin\omega_o) \tag{8d}$$

$$\Delta\Omega = -\frac{3nJ_{20}R_m^2 \cos i}{2a^2(1-e^2)^2}t - \frac{3nJ_{22}R_m^2 \cos i}{2n_1a^2(1-e^2)^2}(\sin 2\Omega' - \sin 2\Omega_o')$$

$$-\frac{J_{30}R_m e \cos i}{2aJ_{20}(1-e^2)\sin i}(\cos\omega - \cos\omega_o) \qquad (8e)$$

The elements a, e, and i that appear in the coefficients above, strictly speaking, are mean values as discussed in appendix A.

Most of the angular quantities in the preceding equations are illustrated in figure 1. In the following discussion perturbations of differing durations are discussed. Perturbing terms involving true anomaly v are said to cause short-period effects since these effects are periodic with a period equal to that of the satellite in its orbit. Perturbing terms containing the longitude of nodes relative to the mean earth-moon line Ω' are said to cause long-period effects which have a period approximately equal to half the period of the moon's rotation about its polar axis. Terms involving the argument of pericentron ω are said to cause long-period effects which have a period equal to the period of the line of apsides of the lunar satellite orbit. Perturbing terms which are independent of the angles v, Ω', and ω are referred to as secular effects. These effects are permanent and, as such, have an infinite period. In the expressions for the variations in the elements given by equations (8), the short-period effects have been averaged out leaving only the secular and both long-period effects. The changes in the elements due to short-period effects are, in general, much smaller than the long-period and secular effects and will be considered in a later section of this paper.

As indicated in equations (8), the mass anomalies cause no first-order perturbations in the semimajor axis. The arguments of pericentron and longitude of node, however, have perturbations due to all three effects; that is, oblateness, equatorial ellipticity, and pear-shape. The effect of the oblateness (J_{20} term) on these two elements is a secular change. The effects of equatorial ellipticity and pear-shape (J_{22} and J_{30} terms) take the form of long-period changes. The eccentricity has only a long-period change caused by the pear-shape effect. The change in inclination is due to both long-period effects - equatorial ellipticity and pear-shape.

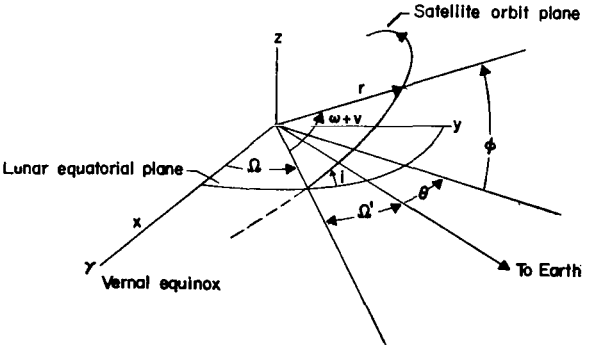

Figure 1.- Illustration of pertinent angles.

Variation in Pericentron Altitude

In a study of close-lunar satellite lifetimes, the main concern is the manner in which the pericentron altitude changes with time. For an orbit in

which the semimajor axis is constant (for instance, when mass anomalies cause the perturbations and with short-period effects neglected), the change in pericentron altitude is given by

$$\Delta r_p = -a\,\Delta e \tag{9}$$

A first-order approximate analysis can be performed on the satellite lifetime with the change in eccentricity, given by equation (8b), substituted into equation (9) which gives

$$\left.\begin{aligned} \Delta r_p &= \frac{1}{2}\frac{J_{30}}{J_{20}} R_m \sin i(\sin\omega - \sin\omega_o) \\ t &= -\frac{\omega_o}{\dot{\omega}} + \frac{1}{\dot{\omega}} \sin^{-1}\left(\frac{2J_{20}\,\Delta r_p}{J_{30}R_m \sin i} + \sin\omega_o\right) \end{aligned}\right\} \tag{10}$$

If the expression for $d\omega/dt$ obtained in appendix A is used, the variation in Δr_p with time can be obtained. It is shown in appendix A that an approximate expression for $d\omega/dt$ is given by

$$\frac{d\omega}{dt} \approx \frac{3nJ_{20}R_m^2}{a^2(1 - e^2)^2}\left(1 - \frac{5}{4}\sin^2 i\right) \tag{11}$$

The main analysis will be made (with the exception of a comparison of lifetimes using first- and second-order results) by utilizing the first-order results of equations (10) and (11).

A second-order expression for Δr_p is developed in appendix B. This result is obtained by assuming $d\omega/dt$ is given by the sum of the secular and long-period terms, that is

$$\frac{d\omega}{dt} = \frac{3nJ_{20}R_m^2}{a^2(1 - e^2)^2}\left(1 - \frac{5}{4}\sin^2 i\right)\left[1 + \frac{J_{30}R_m \sin\omega}{2J_{20}a(1 - e^2)}\,\frac{\sin^2 i - e^2\cos^2 i}{e \sin i}\right] \tag{12}$$

The result of this analysis is that Δr_p, including second-order terms, is given as

$$\Delta r_p = \frac{J_{30}R_m \sin i}{2fJ_{20}} \log\left(\frac{1 + f \sin\omega}{1 + f \sin\omega_o}\right) \tag{13}$$

where

$$f = \frac{J_{30}R_m}{2J_{20}a(1 - e^2)}\,\frac{\sin^2 i - e^2\cos^2 i}{e \sin i} \tag{14}$$

Analysis of Short-Period Perturbations and Earth Effects

The short-period variations in the elements due to the lunar oblateness are developed in reference 4. In the notation of the present analysis, the short-period variations of semimajor axis and eccentricity are written as

$$(\Delta a)_1 = \frac{3R_m^2}{2a} J_{20}\left\{\frac{2}{3}\left(1 - \frac{3}{2}\sin^2 i\right)\left[\left(\frac{a}{r}\right)^3 - \left(1 - e^2\right)^{-3/2}\right] + \left(\frac{a}{r}\right)^3 \sin^2 i \cos 2(\omega + v)\right\}\Bigg|_{v_o}^{v} \tag{15}$$

$$(\Delta e)_1 = \frac{1 - e^2}{e}\frac{3J_{20}}{2a^2}\left\{\frac{1}{3}\left(1 - \frac{3}{2}\sin^2 i\right)\left[\left(\frac{a}{r}\right)^3 - \left(1 - e^2\right)^{-3/2}\right]\right.$$

$$\left. + \frac{1}{2}\left(\frac{a}{r}\right)^3 \sin^2 i \cos 2(\omega + v)\right\}\Bigg|_{v_o}^{v} - \frac{3\sin^2 i J_{20}}{4a^2 e\left(1 - e^2\right)}\left[\cos 2(\omega + v)\right.$$

$$\left. + e\cos(v + 2\omega) + \frac{1}{3}e\cos(3v + 2\omega)\right]\Bigg|_{v_o}^{v} \tag{16}$$

The change in the pericentron altitude due to these short-period variations is obtained by substitution of equations (15) and (16) into the following expression for $\left(\Delta r_p\right)_1$:

$$\left(\Delta r_p\right)_1 = (1 - e)(\Delta a)_1 - a(\Delta e)_1 \tag{17}$$

The variations in the pericentron altitude of the lunar orbit, due to the disturbing effect of the earth, can be computed from the following equations. The mean rates (over a lunar day) of argument of pericentron, eccentricity, and semimajor axis due to the influence of the earth are:

$$\left(\frac{d\omega}{dt}\right)_E = \frac{3n_1}{2n}\sqrt{1 - e^2}\left[1 + \frac{5\sin^2\omega\left(e^2 - \sin^2 i\right)}{2\left(1 - e^2\right)}\right] \tag{18}$$

$$\left(\frac{de}{dt}\right)_E = \frac{15}{8}\frac{n_1^2}{n}e\sqrt{1 - e^2}\sin^2 i \sin 2\omega \tag{19}$$

$$\left(\frac{da}{dt}\right)_E = 0 \tag{20}$$

For close-lunar satellites moderately inclined, $\left(\frac{d\omega}{dt}\right)_E$ is small compared with $\dot{\omega}_s$. If $d\omega/dt$ is approximated by $\dot{\omega}_s$, then equation (19) can be integrated to obtain $(\Delta e)_E$ as:

$$(\Delta e)_E = -\frac{15n_1^2}{16n\dot{\omega}_s} e\sqrt{1 - e^2} \sin^2 i(\cos 2\omega - \cos 2\omega_o) \tag{21}$$

Substitution of equation (21) into equation (19) gives for $(\Delta r_p)_E$ the following expression:

$$(\Delta r_p)_E = \frac{15}{16} \frac{an_1^2}{n\dot{\omega}_s} e\sqrt{1 - e^2} \sin^2 i(\cos 2\omega - \cos 2\omega_o) \tag{22}$$

From equation (22) it can be deduced that the maximum decrease in the pericentron altitude due to earth effects is

$$\left[(\Delta r_p)_E\right]_{max} = -\frac{15}{16} \frac{a}{n} \frac{n_1^2}{\dot{\omega}_s} e\sqrt{1 - e^2} \sin^2 i \left[1 + \left|\cos 2\omega_o\right|\right] \tag{23}$$

The maximum value of $\left[(\Delta r_p)_E\right]_{max}$ occurs for $\omega_o = 0^\circ$ or 180°, and is

$$\left[(\Delta r_p)_E\right]_{max} = -\frac{15}{8} \frac{a}{n} \frac{n_1^2}{\dot{\omega}_s} e\sqrt{1 - e^2} \sin^2 i \tag{24}$$

LUNAR SATELLITE LIFETIME STUDY

Lifetime Analysis

In this analysis the lifetime of a close-lunar satellite is considered ended whenever the altitude of pericentron decreases more than a specified amount which depends on the initial pericentron altitude. For instance, the lifetime of an orbit with an initial altitude of pericentron of 46 kilometers might be considered ended whenever the decrease in r_p is more than 36 kilometers, that is, when $\Delta r_p = -36$ kilometers. This criterion on lifetime would allow a 10-kilometer variation in pericentron altitude which may be present as a result of a combination of effects neglected in the analysis such as second-order effects in ω, short-period perturbations, and perturbations due to the earth.

The first-order analysis on the lifetime of the satellite is obtained from a solution of equations (10) and (11) which are repeated here.

$$\Delta r_p = \frac{1}{2}\frac{J_{30}}{J_{20}} R_m \sin i(\sin \omega - \sin \omega_o)$$

$$\frac{d\omega}{dt} \approx \frac{3nJ_{20}R_m^2}{a^2(1 - e^2)^2}\left(1 - \frac{5}{4}\sin^2 i\right)$$

In all examples the orbit used (unless otherwise noted) is a direct orbit for which the pericentron and apocentron altitudes are 46 and 925 kilometers, respectively. (Apocentron is defined as the point in the orbit of one body about another at which the greatest separation of the two bodies occurs.) The inclination is 21° and the initial location of the node is 50° west of the mean earth-moon line $(\Omega_o' = -50°)$. This situation corresponds to a typical earth-moon transfer trajectory for which the transit time is about 80 hours. The magnitude of J_{30} is assumed to be 9.3×10^{-5}. A parametric study on both inclination and J_{30} is performed.

The variation in r_p with time as given by equations (10) and (11) is illustrated in figure 2 for a negative sign on J_{30}. The effect of some initial values of the argument of pericentron is illustrated. A plus sign for J_{30} simply causes a change of sign on the values presented in figure 2. These curves indicate that the pericentron altitude can either increase or decrease initially depending on the values of ω_o and J_{30} that are used.

A solution for the satellite lifetime T from equations (10) and (11) is illustrated in figure 3 for a range of ω_o from 0° to 360°. Several interesting features are present in this figure. With $J_{30} = -9.3 \times 10^{-5}$, a minimum lifetime of about 2 weeks occurs for ω_o near 0° and infinite lifetimes occur for the range $48° < \omega_o < 132°$. A similar situation exists for $J_{30} = 9.3 \times 10^{-5}$: a minimum lifetime of 2 weeks occurs for ω_o near 180°, and an infinite lifetime occurs for $228° < \omega_o < 312°$.

The explanation for the shift from a finite to an infinite lifetime can be obtained from figure 4. For $\omega_o < 48°$, for instance $\omega_o = 30°$, the curve intersects the line marked $\Delta r_p = -36$ kilometers after about 16 days; hence, a 16-day lifetime is shown in figure 3. The curve for $\omega_o = 48°$ is tangent to the line marked $\Delta r_p = -36$ kilometers after

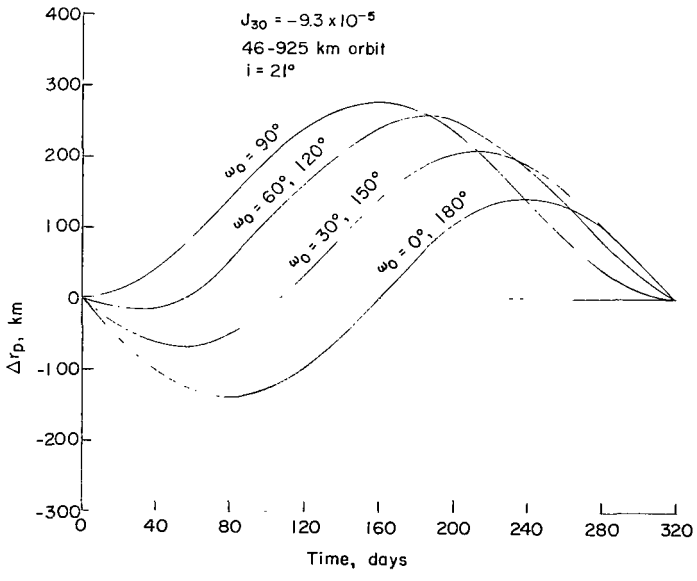

Figure 2.- Variation of Δr_p with time for several initial values of the argument of pericentron.

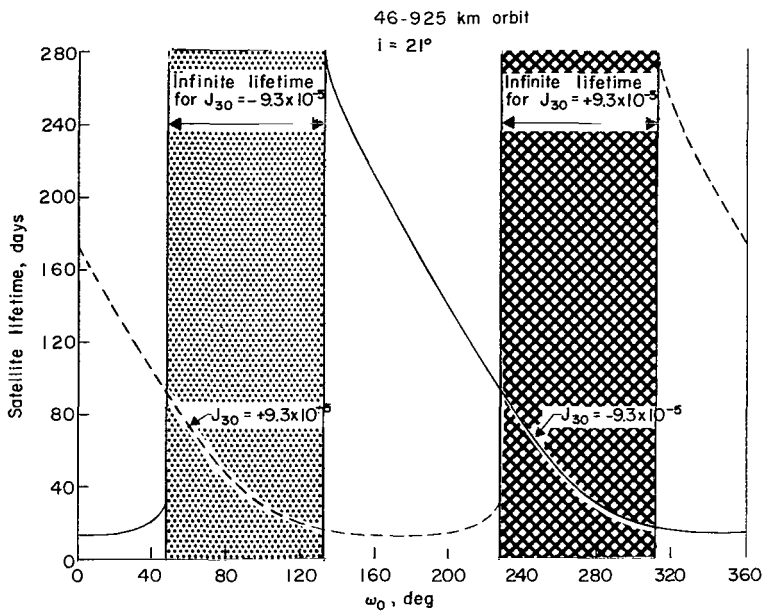

Figure 3.- Satellite lifetime as a function of initial values of argument of pericentron.

about 35 days so that this time serves as a limiting value of the finite lifetimes for $\omega_0 < 48^\circ$. For $48^\circ < \omega_0 < 132^\circ$, for instance $\omega_0 = 60^\circ$, the curve never intersects the line marked $\Delta r_p = -36$ kilometers; hence, the infinite lifetime.

The estimate of the magnitude of J_{30} of 9.3×10^{-5} provides a possible basis for determination of the magnitude of the pericentron altitude variations. However, the sign of J_{30} is very critical to the actual lifetime of the satellite. Since the sign is unknown, it is natural to inquire into the possible existence of initial conditions on the satellite that result in "optimum" or favorable lifetimes for a given magnitude of J_{30} regardless of its sign. Reference to figure 3 indicates that for $|J_{30}| = 9.3 \times 10^{-5}$ there is an initial value of the argument of pericentron of approximately 48° for which the lifetime is infinite if $J_{30} < 0$ and is favorable ($T = 95$ days) if $J_{30} > 0$. The finite value is called the "optimum lifetime." A satellite in an orbit having this initial value of argument of pericentron will have at least a lifetime of 95 days. A similar situation exists at $\omega_0 = 228^\circ$. For the remainder of the analysis, when optimum lifetimes are considered, the initial value of argument of pericentron less than 90° will be used and referred to as $(\omega_0)_m$. It should be noted that $(\omega_0)_m = 48^\circ$ was for the special

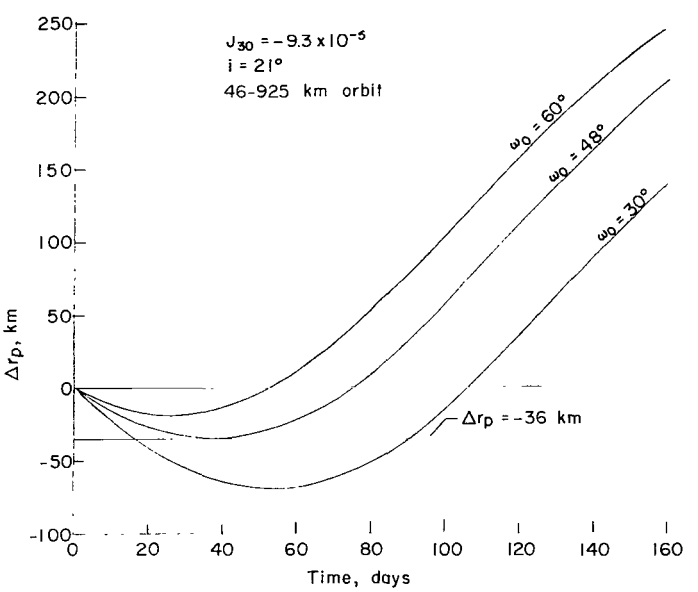

Figure 4.- Illustration of infinite and finite lifetimes concept.

case of $i = 21^{\circ}$ and $|J_{30}| = 9.3 \times 10^{-5}$. In general $(\omega_o)_m$ is dependent on both inclination and $|J_{30}|$.

Photographic Mission

A lunar photographic mission to be performed by a satellite in a close-lunar orbit should be designed so that the orbit has a sufficiently low pericentron altitude to provide good photographic resolution. At the same time, the pericentron altitude must be sufficiently high so that the satellite lifetime is not ended before the photographic mission is completed. Other characteristics of the orbit such as eccentricity, inclination, and initial argument of pericentron must also be chosen properly since they affect the lifetime of the satellite as well as the photographic coverage of the lunar surface. The value of initial argument of pericentron greatly affects the lifetime of the satellite and the area available for the photographic mission. For this reason it is chosen to correspond to the value that results in the optimum lifetime, discussed previously.

Another factor to be considered in a photographic mission is that of favorable lighting conditions. The lighting conditions on a region are considered favorable for photography whenever the sun rays are at about 60° to the local vertical. This situation is illustrated in figure 5. As shown in figure 5, the initial argument of pericentron should be situated near the point where the trace of the lunar satellite plane intersects the 60° circle centered about a line in the direction of the sun. These conditions will insure favorable lighting for the photographic phase of the mission.

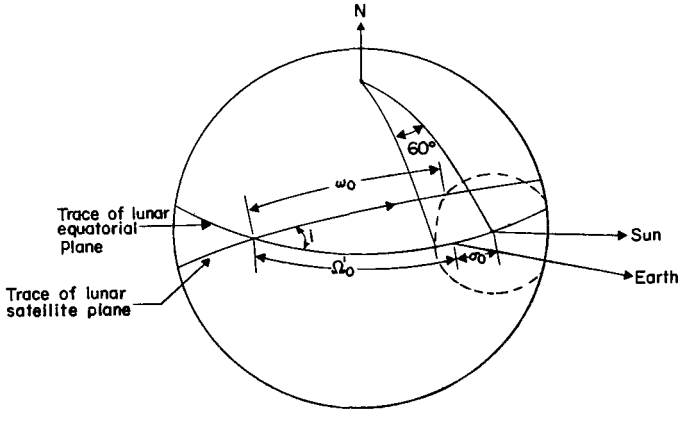

Figure 5.- Illustration of initial angular relationship for photographic mission.

Effect of Orbit Inclination on Target Site Selections and Lifetimes of Close-Lunar Satellites

Utilization of the optimum lifetime (previously defined) in a lunar mission automatically constrains any operation dependent on the initial value of the argument of pericentron. In the case of a close-lunar photographic mission in which the pictures are to be taken at pericentron, this constraint takes the form of a restriction in surface areas available for the experiment. This constraint, however, can be made less severe by allowing some freedom in the selection of the inclination for the mission. The effect of inclination on changes in pericentron altitude, optimum lifetimes, initial latitudes and longitudes of pericentron location, and subsequent changes with time, initial solar positions, and initial values of $(\omega_o)_m$ is considered in this section. In all cases, the orbits considered are direct and have pericentron and apocentron altitudes of 46 and 925 kilometers and $\Omega_o' = -50^o$. The values of $(\omega_o)_m$ were determined from the assumption that the life of the satellite ended whenever the pericentron altitude decreased more than 36 kilometers.

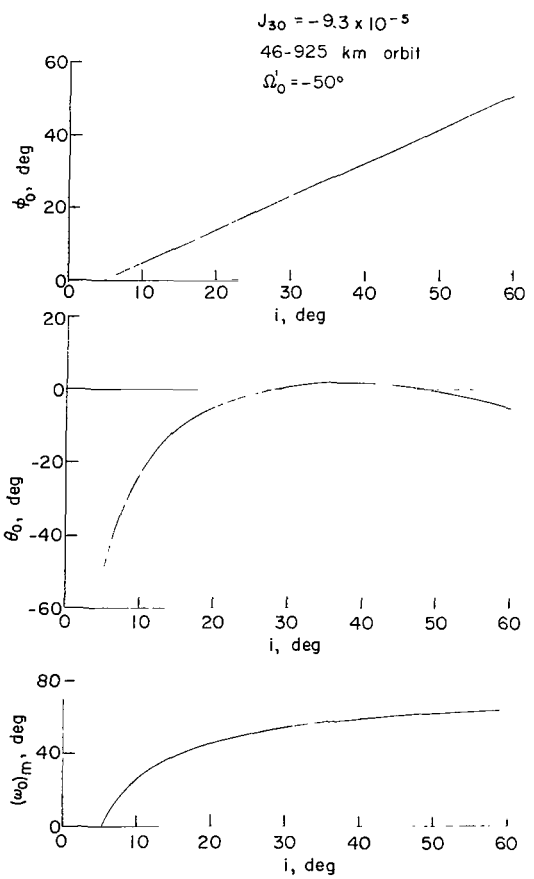

Figure 6.- Initial values of argument of pericentron.

The condition needed to obtain an expression for $(\omega_o)_m$ can be deduced from the definition of $(\omega_o)_m$ and from reference to figure 4. It can be seen from this figure that $\omega_o = (\omega_o)_m$ whenever the conditions $\frac{d}{dt}(\Delta r_p) = 0$ and $\Delta r_p = -36$ kilometers occur together. If this operation is performed on equation (10) and if the value of $\Delta r_p = -36$ kilometers is used in equation (10) it is found that

$$(\omega_o)_m = \sin^{-1}\left(\frac{-72J_{20}}{|J_{30}|R_m \sin i} + 1\right) \qquad (25)$$

The dependence of $(\omega_o)_m$ on i as determined from equation (25) is shown in figure 6. The maximum value of $(\omega_o)_m$ for $J_{30} = -9.3 \times 10^{-5}$ is about 65^o corresponding to $i = 90^o$. The minimum value is 0^o and occurs for $i = 5^o$. For inclinations less than about 5^o, the lifetime of the satellite is unaffected by the presence of a J_{30} term of this magnitude. Figure 6 also illustrates the variation of initial latitude and longitude of pericentron location with inclination. Note that these initial longitudes and latitudes are

essentially restricted to the northwest (cartographic) quadrant of the moon. Other areas are possible if a different direction in orbit is considered.

The change in pericentron altitude with time, for various inclinations, is shown in figure 7. These curves were generated with $\omega_o = (\omega_o)_m$ and $J_{30} = -9.3 \times 10^{-5}$. Note that Δr_p is never less than -36 kilometers since, according to figure 3, these values of J_{30} and $\omega_o = (\omega_o)_m$ cause an infinite lifetime. However, if a value of $J_{30} = 9.3 \times 10^{-5}$ were used, the curve in figure 7 would be inverted and, for $\omega_o = (\omega_o)_m$, an infinite lifetime would not occur. (See fig. 3 for the case of $i = 21^\circ$.) Instead, the optimum lifetimes which occur are, for example, 104 days for $i = 15^\circ$, and 124 days for $i = 10^\circ$.

Figure 8 presents the variation in the optimum lifetime with inclination. Inclinations of less than about 5° result in an infinite lifetime. Inclinations greater than 5° result in finite optimum lifetimes. The minimum of the optimum lifetime, about 95 days, occurs for an inclination near 25°.

The initial rate of change of the pericentron altitude for $\omega_o = (\omega_o)_m$ and $J_{30} = -9.3 \times 10^{-5}$ is also shown in figure 8. For $5^\circ < i < 60^\circ$, the pericentron decreases initially. For $5^\circ < i < 15^\circ$, this decrease continues until about 45 days have passed, as can be seen from figure 7. The initial rate of change in pericentron altitude for $i = 10^\circ$ and 15° is -1.3 and -1.7 kilometers/day, respectively. Figure 7 indicates that these rates remain approximately constant for the first 10 days in orbit. These rates indicate that in addition to the provision of optimum lifetimes, the

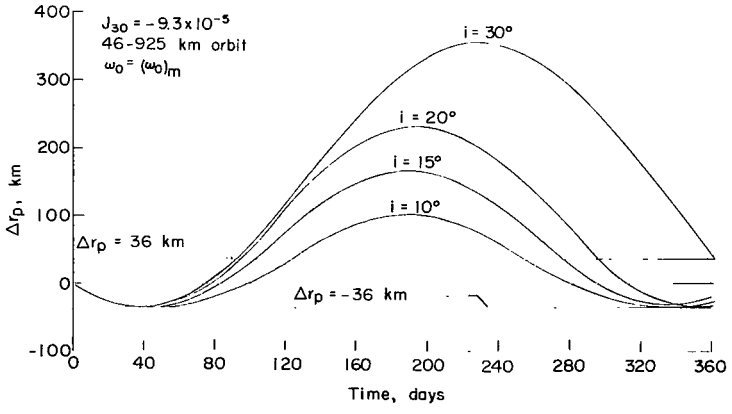

Figure 7.- Variation of pericentron altitude with time.

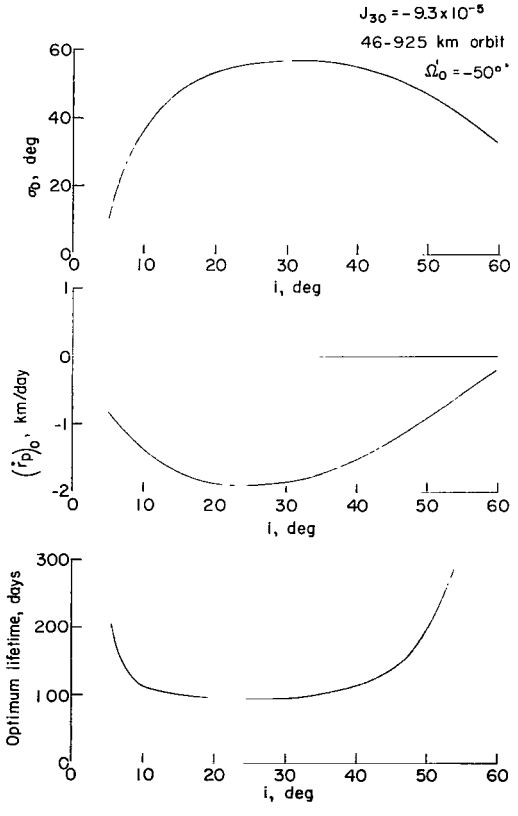

Figure 8.- Initial values of r_p and σ and optimum lifetimes.

condition $\omega_o = (\omega_o)_m$ causes changes in the pericentron altitude that could reveal, through an analysis of the tracking data, an early determination of the sign of J_{30} and a first estimate of its magnitude.

The initial solar position σ_o is also shown in figure 8. An initial longitude of node $\Omega_o' = -50^\circ$ and solar incidence angle of 60° to the local vertical were used in the determination of the solar positions. The value of σ_o varies from 10° east to about 57° east for inclinations between 5° and 30°. These angles correspond to about 1 and $4\frac{1}{2}$ days before full moon. Reference to figure 5 indicates that it is also possible to obtain favorable lighting conditions for these initial elements after full moon. The values of σ_o in figure 8 and the values of ϕ_o and θ_o in figure 6 were computed by use of equations (C2) and (C3) from appendix C.

The pericentron locations, latitude and longitude, are shown in figure 9 as a function of time after orbit establishment. Figure 9 shows that both ϕ and θ essentially change linearly with time; the rate of change in ϕ is much less than that in θ. A corresponding plot of surface coverage is shown in figure 10. Note that the constraint of optimum lifetime has made unavailable, to a photographic mission, the greater part of regions in the immediate vicinity of the lunar equator. A means of including this region, however, could be obtained by such operations as a delay in orbit or a simple plane-change technique.

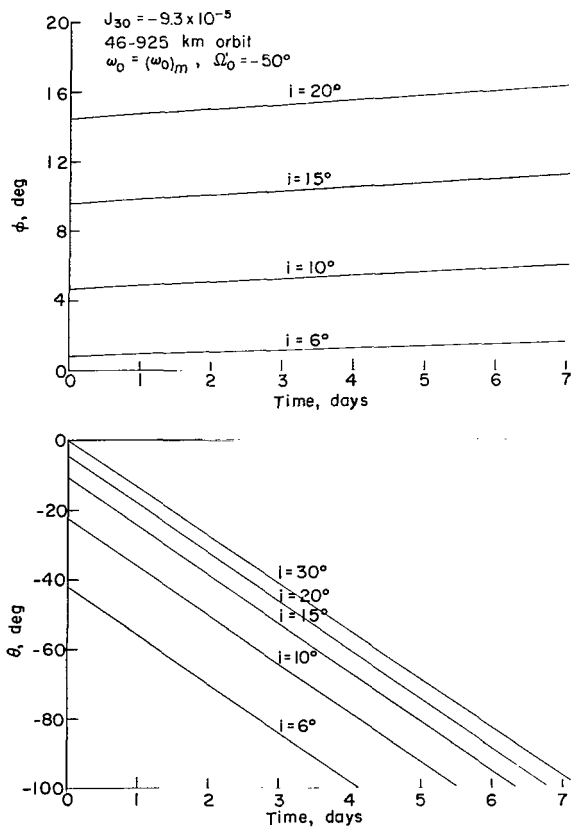

Figure 9.- Variation of pericentron location with time after orbit establishment.

Effect of the Magnitude of J_{30} on the Lifetime of a Close-Lunar Satellite

The previous analysis was performed by using the value $J_{30} = -9.3 \times 10^{-5}$. Since this value is only a first estimate of J_{30}, it is of interest to investigate some of the previous results when other values of J_{30} are assumed. The effect of J_{30} on such parameters as $(\Delta r_p)_{max}$, $(\omega_o)_m$, optimum lifetimes, $(\dot{r}_p)_o$, and pericentron location are shown in figures 11 to 13. The values of J_{30} used are the suggested value

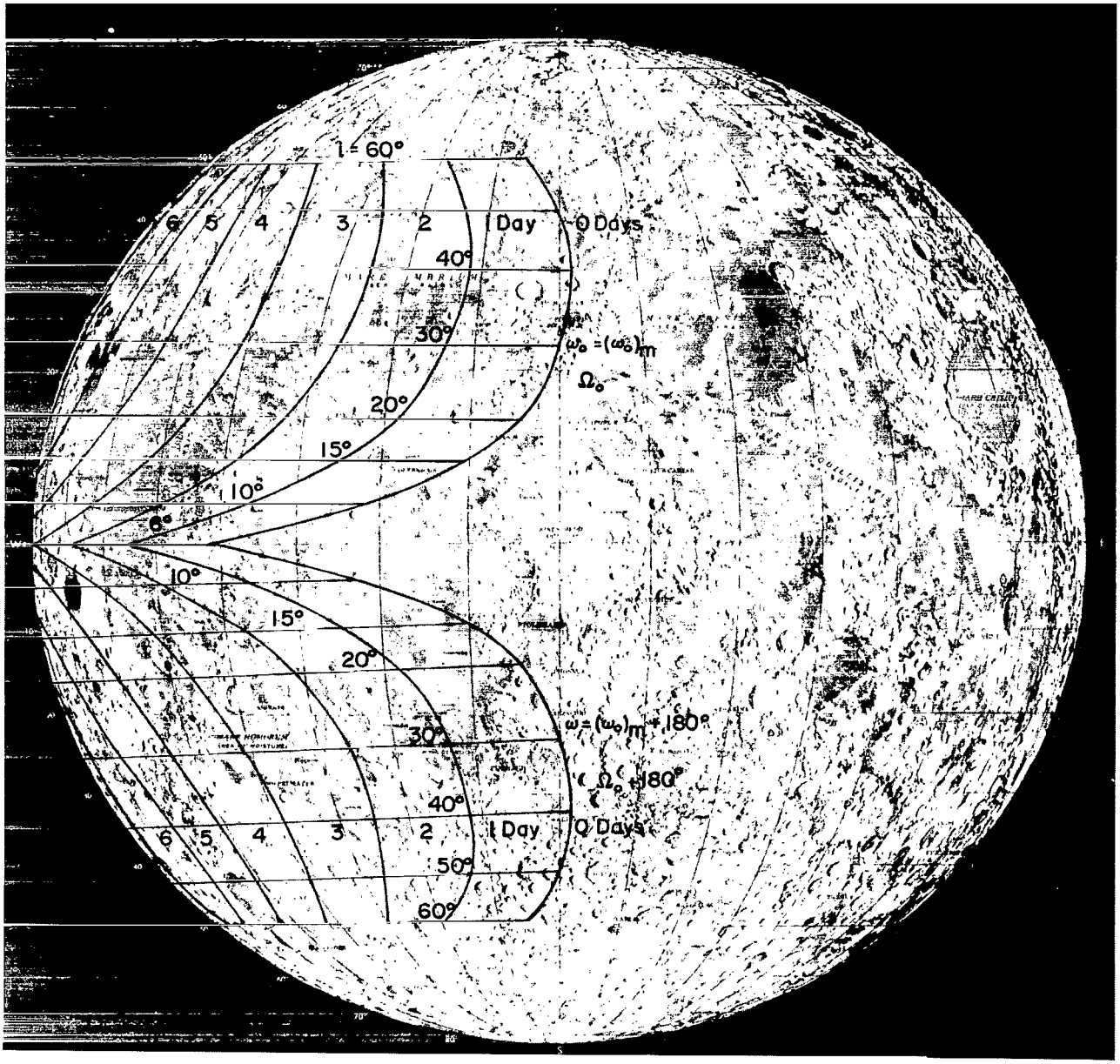

L-64-1018

Figure 10.- Trace on Moon of argument of pericentron with time.

of 9.3×10^{-5}, twice this value, one-half this value, and one-fourth this value. In all cases $\omega_0 = (\omega_0)_m$.

Figure 11 indicates that there are certain values of inclination, depending on the value of J_{30}, for which $(\omega_0)_m$ is zero; values of i below these correspond to indefinite lifetimes for the satellite. In general, the inclination for $(\omega_0)_m = 0$ decreases with an increase in magnitude of J_{30}. Equatorial orbits (i = 0°) were not considered in the analysis since one requirement of the mission is the determination of a value for J_{30}. Figure 13 gives the location of the pericentron for the first week after establishment of the lunar satellite corresponding to three values of J_{30} and i = 15°. For a variation in J_{30} from -4.65×10^{-5} to -18.6×10^{-5}, a change in $(\omega_0)_m$ occurs which causes the initial latitude of pericentron to change from about 4° to about 11°. The corresponding changes in initial longitude of the pericentron are from -34° to 4°.

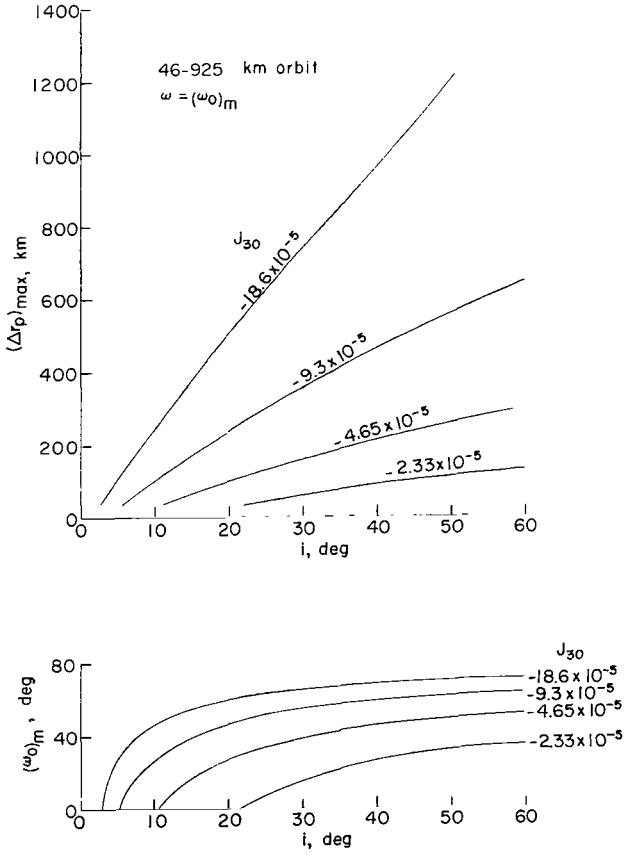

Figure 11.- Variation of $(\Delta r_p)_{max}$ and $(\omega_0)_m$ with inclination.

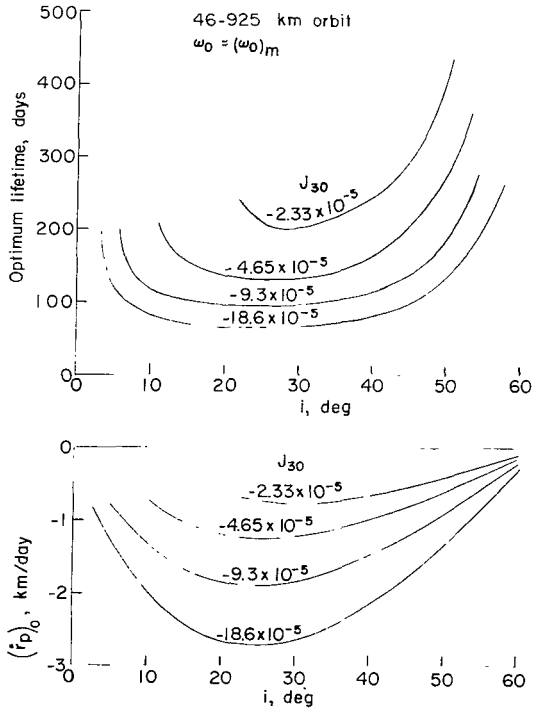

Figure 12.- Variation of $(\dot{r}_p)_0$ and optimum lifetime with inclination.

INFLUENCE OF SECOND-ORDER EFFECTS, SHORT-PERIOD PERTURBATIONS, AND EARTH EFFECTS

Second-Order Effects

The second-order effects of J_{30} on the lifetime of the lunar satellite are determined from equations (12) to (14). These effects are dependent on the magnitude of the correction function f given by equation (14). This function is seen to be dependent on a, e, i, J_{20}, J_{30}, and R_m. For a given orbit size and assumed lunar gravitational potential, the value of f varies with i as shown in figure 14. In the vicinity of $i = 10^o$, second-order effects are negligible but may become important at lower and higher inclinations. The effect of this correction on the lifetime of a satellite is shown in figure 15. In general, the lifetime decreases with the greatest effect (a 20-day difference) near $\omega_o = 180^o$. The band of values of ω_o for which the satellite has an infinite lifetime also narrows.

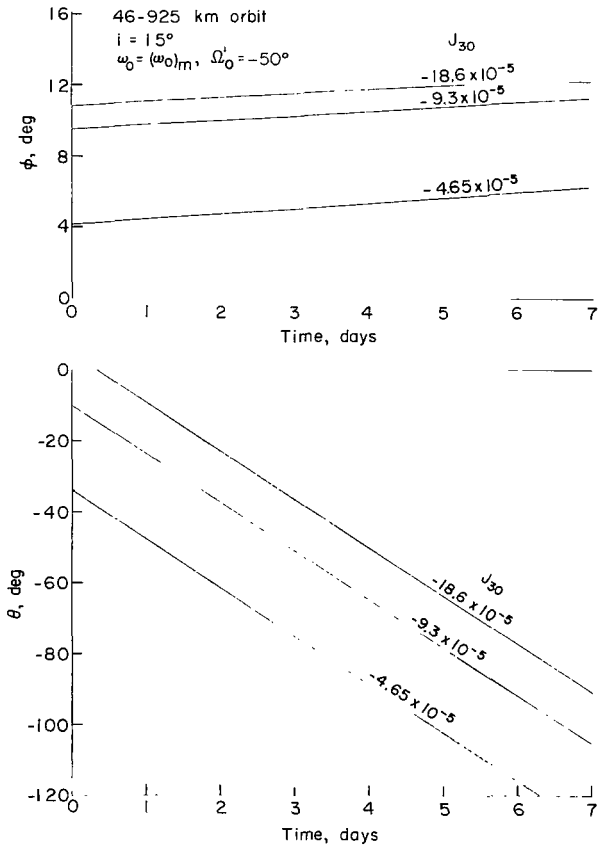

Figure 13.- Variation of pericentron location with time for various values of J_{30}.

Short-Period Perturbations and Earth Effects

Some results for short-period change in pericentron altitude are computed from equations (15) to (17) and are shown plotted in figure 16. The change in pericentron altitude from the time the satellite is at some

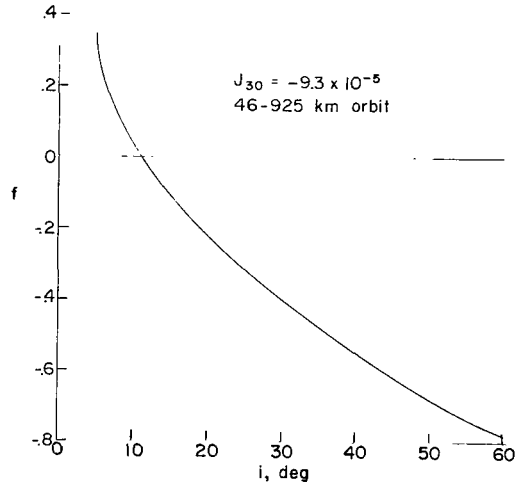

Figure 14.- Maximum effect of correction to ω with inclination.

initial point in the orbit $v = v_0$ to the time it is at pericentron $v = 0^\circ$ is shown for all possible initial true anomalies. Two initial arguments of pericentron are considered, $\omega_0 = 0^\circ$ and $\omega_0 = 40^\circ$ for each of two orbits: one having a pericentron of 46 kilometers and an apocentron of 925 kilometers, the other having a pericentron of 46 kilometers and an apocentron of 1850 kilometers. The largest decrease in pericentron altitude (less than 0.6 kilometer for these orbits) occurs for an initial location of the satellite in the vicinity of apocentron $(v_0 = 180^\circ)$. These variations in pericentron altitude are small compared with the long-period variations obtained by assuming the suggested magnitude of 9.3×10^{-5} for J_{30}.

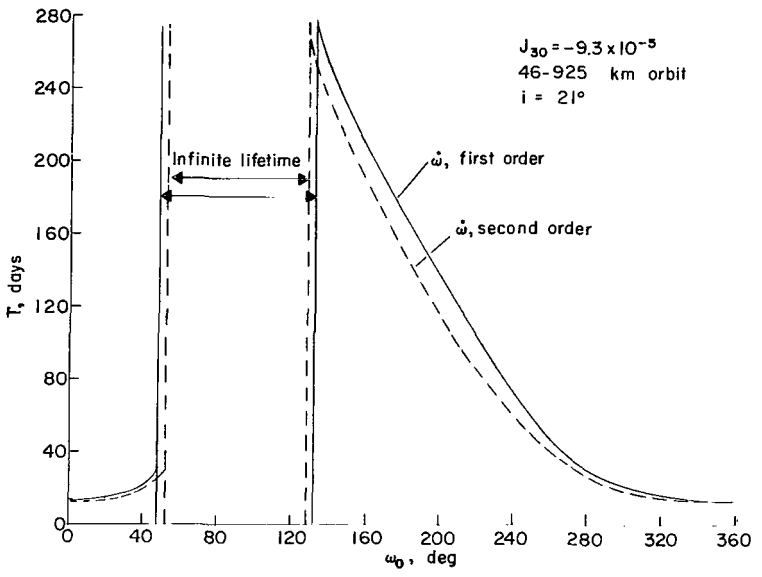

Figure 15.- Comparison of lifetimes for first- and second-order analysis.

The effect of the earth on the lifetime of a close-lunar orbit can be determined from equations (18) to (24). In figure 17, the variation in the pericentron altitude with time due to the earth effects is shown. The maximum decrease in the pericentron altitude for these initial arguments of pericentron is about 5.0 kilometers. The maximum value of $\left[(\Delta r_p)_E\right]_{max}$ is given by equation (24) as a function of inclination for a given orbit size. This value is shown plotted in figure 18 against i for a 46-925- and a 46-1850-kilometer orbit. For these orbits it can be seen that the maximum value of $\left[(\Delta r_p)_E\right]_{max}$ lies in the range from 0 to 70 kilometers for inclination between 0° and 50°. For the 21° inclined orbit the average values

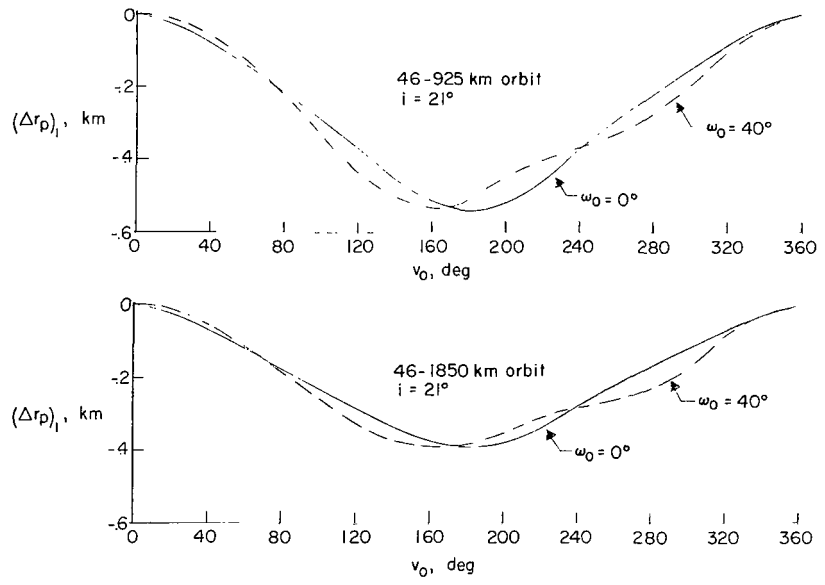

Figure 16.- Short periodic variation in pericentron altitude with time.

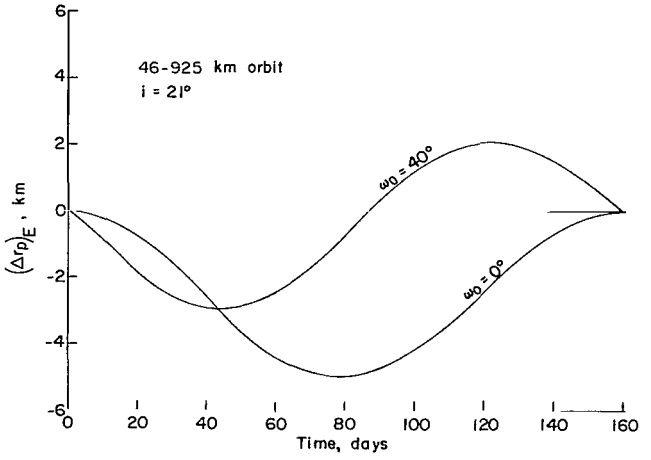

Figure 17.- Variation of pericentron altitude with time due to earth effects.

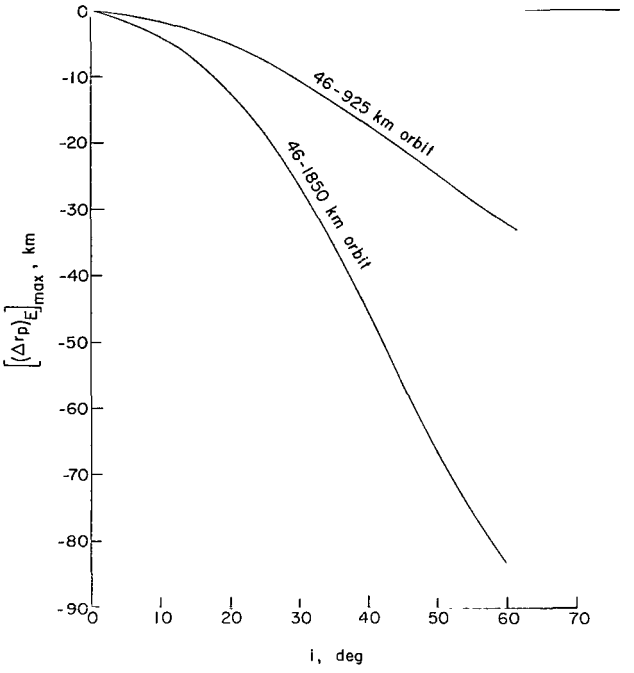

Figure 18.- Maximum change in pericentron altitude due to earth effects.

of the maximum change in pericentron altitude due to earth effects on these orbits are about 6 and 14 kilometers. These results indicate that both the short-period and earth perturbations on the pericentron altitude of low inclined close-lunar satellite orbits are small compared with the previously discussed long-period effects but can become significant for more inclined and larger orbits.

CONCLUDING REMARKS

An analytical lifetime study of close-lunar satellites has been performed for a mathematical model of the moon which has oblateness, equatorial ellipticity, and a nonsymmetric distribution of mass in the northern and southern hemispheres. It is shown that a value of the coefficient of the third zonal harmonic J_{30} for the moon of approximately 36 times that for the earth can cause large changes in the pericentron altitude resulting, in many instances, in short lifetimes of close-lunar satellites. On the other hand, it is shown that there are conditions for which the lifetime is indefinite for a favorable sign of J_{30}.

In general, an arbitrary initial argument of pericentron either results in a long lifetime if J_{30} has one sign or a short lifetime if J_{30} is of the opposite sign. However, it is shown that, associated with each orbit, there are two initial arguments of pericentron, $(\omega_0)_m$ and $(\omega_0)_m + 180^\circ$, for which the lifetime is relatively long independent of the sign of J_{30}. Utilization of these "optimum lifetimes" in a lunar mission automatically constrains any

operation dependent on the initial value of the argument of pericentron. It is found that, in the case of a close-lunar photographic mission in which pictures are to be taken at pericentron, this constraint takes the form of a restriction on the lunar-surface coverage available for the experiment. However, this restriction can be lifted somewhat by allowing some freedom in the choice of orbit inclination for the mission. Under this restriction, the region at the center of the lunar disk is unavailable for immediate photographic coverage in a typical close-lunar orbit.

It is shown that the constraint of optimum lifetimes allows a great deal of freedom in selecting photographic surface areas and a means of obtaining data on the lunar gravitational field from a tracking analysis. The magnitude of the time rate of change of the pericentron altitude should be sufficiently large for this condition to obtain a first estimate of the magnitude of J_{30} as well as its sign.

The general results of the analysis are based on satellite lifetimes as determined from a secular change in the argument of pericentron. The lifetimes as determined by a more accurate representation of the change in argument of pericentron, a secular plus a long-period change, is considered briefly. The result of the calculations indicated that the more accurate analysis results in shorter lifetimes.

Results of an analysis of short-period perturbations and earth effects indicated that the lunar satellite lifetime is not affected, to a great extent, by these factors whenever the orbits are moderately inclined and are not too large.

Langley Research Center,
National Aeronautics and Space Administration,
Langley Station, Hampton, Va., March 15, 1965.

APPENDIX A

PERTURBATION OF THE ELEMENTS

Analyses similar to the following ones are performed in numerous papers. (See, for example, ref. 4.) The intent here, however, is to give some of the details not present in the other developments.

The gravitational potential function used to represent the moon in this analysis is

$$U(r,\theta,\phi) = \frac{\mu}{r}\left[1 + \frac{R_m^2}{2r^2} J_{20}\left(1 - 3\sin^2\phi\right) - \frac{3R_m^2}{r^2} J_{22}\cos^2\phi\cos 2\theta - \frac{R_m^3}{2r^3} J_{30}\sin\phi\left(5\sin^2\phi - 3\right)\right] \qquad (A1)$$

The disturbing function due to the fact that the moon has mass anomalies is

$$R = U - \frac{\mu}{r} = \frac{\mu R_m^2}{r^3}\left[\frac{J_{20}}{2}\left(1 - 3\sin^2\phi\right) - 3J_{22}\cos^2\phi\cos 2\theta - \frac{R_m}{2r} J_{30}\sin\phi\left(5\sin^2\phi - 3\right)\right] \qquad (A2)$$

The disturbing function R can be expressed in terms of the elements of the orbit from a consideration of the following sketch:

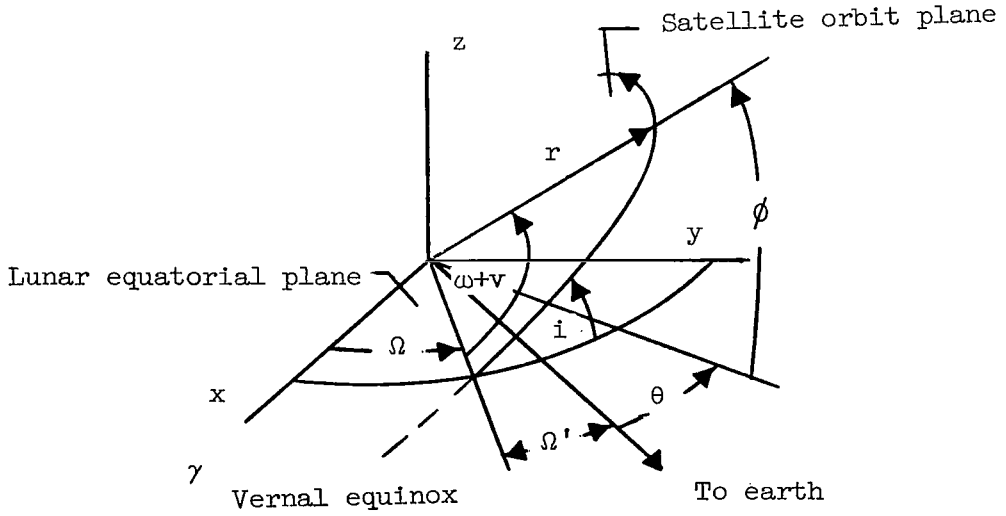

APPENDIX A

Application of spherical trigonometry to the geometry presented in the sketch gives

$$\cos\theta = \frac{1}{\cos\phi}\left[\cos(\omega + v)\cos\Omega' - \cos i \sin\Omega'\sin(\omega + v)\right] \tag{A3}$$

From this expression the term $\cos^2\phi \cos 2\theta$ in equation (A2) can be expressed as

$$\cos^2\phi \cos 2\theta = \frac{1}{2}\left[\left(1 + \cos^2 i\right)\cos 2\Omega'\cos 2(\omega + v) + \sin^2 i \cos 2\Omega' - 2 \cos i \sin 2\Omega'\sin 2(\omega + v)\right] \tag{A4}$$

In terms of the elements of the orbit, R can be written as

$$R = \frac{\mu R_m^2}{a^3}\left(\frac{a}{r}\right)^3\left\{\frac{J_{20}}{4}\left[2 - 3 \sin^2 i + 3 \sin^2 i \cos 2(\omega + v)\right] - \frac{3J_{22}}{2}\left[\left(1 + \cos^2 i\right)\cos 2\Omega'\cos 2(\omega + v) + \sin^2 i \cos 2\Omega' - 2 \cos i \sin 2\Omega'\sin 2(\omega + v)\right] - \frac{J_{30}R_m}{8a}\left(\frac{a}{r}\right)\left[3\left(5 \sin^2 i - 4\right)\sin(\omega + v) - 5 \sin^2 i \sin 3(\omega + v)\right]\sin i\right\} \tag{A5}$$

To eliminate the short periodic perturbations (on the order of one orbital period), integrate R with respect to M from 0 to 2π assuming that a, e, i, ω, and Ω' are constant. This procedure gives, the first order in J_{20}, J_{22}, and J_{30} the following:

$$\bar{R} = \frac{1}{2\pi}\int_0^{2\pi} R\, dM = \frac{1}{2\pi}\int_0^{2\pi} R\left(\frac{r}{a}\right)^2\left(1 - e^2\right)^{-1/2} dv$$

$$= \frac{\mu R_m^2}{a^3}\left[\frac{J_{20}}{2}\left(1 - e^2\right)^{-3/2}\left(1 - \frac{3}{2}\sin^2 i\right) - \frac{3J_{22}}{2}\left(1 - e^2\right)^{-3/2}\sin^2 i \cos 2\Omega' + \frac{3R_m}{2a} J_{30} e\left(1 - e^2\right)^{-5/2}\sin i\left(1 - \frac{5}{4}\sin^2 i\right)\sin\omega\right] \tag{A6}$$

The integration indicated in equation (A6) can be determined immediately if use is made of the following results obtained from reference 5:

$$\left.\begin{aligned} X_o^{n,m} &= \frac{1}{2\pi}\int_0^{2\pi}\left(\frac{r}{a}\right)^n \cos mv\, dM \\ &= (-1)^m\left(\frac{e}{2}\right)^m\left(1-e^2\right)^{n+\frac{3}{2}}\sum_{p=0}^{\infty}\binom{n+m+1+2p}{m+p}\binom{n+1+p}{p}\left(\frac{e}{2}\right)^{2p} \\ \frac{1}{2\pi}&\int_0^{2\pi}\left(\frac{r}{a}\right)^n \sin mv\, dv = 0 \end{aligned}\right\} \qquad (A7)$$

where p is a summation index.

To find the variation in the elements due to this averaged disturbing function $\bar{R}$, the following LaGrange equations are used (ref. 6):

$$\left.\begin{aligned} \frac{da}{dt} &= \frac{2}{na}\frac{\partial \bar{R}}{\partial M} \\ \frac{de}{dt} &= \frac{1-e^2}{na^2e}\frac{\partial \bar{R}}{\partial M} - \frac{\sqrt{1-e^2}}{na^2e}\frac{\partial \bar{R}}{\partial \omega} \\ \frac{d\omega}{dt} &= -\frac{\cos i}{na^2\sqrt{1-e^2}\sin i}\frac{\partial \bar{R}}{\partial i} + \frac{\sqrt{1-e^2}}{na^2e}\frac{\partial \bar{R}}{\partial e} \\ \frac{di}{dt} &= \frac{\cos i}{na^2\sqrt{1-e^2}\sin i}\frac{\partial \bar{R}}{\partial \omega} - \frac{1}{na^2\sin i\sqrt{1-e^2}}\frac{\partial \bar{R}}{\partial \Omega} \\ \frac{d\Omega}{dt} &= \frac{1}{na^2\sqrt{1-e^2}\sin i}\frac{\partial \bar{R}}{\partial i} \end{aligned}\right\} \qquad (A8)$$

Substitution of equation (A6) into equations (A8) gives

$$\frac{da}{dt} = 0 \qquad (A9a)$$

$$\frac{de}{dt} = -\frac{3nR_m^3}{2a^3}\frac{J_{30}\sin i}{\left(1-e^2\right)^2}\left(1-\frac{5}{4}\sin^2 i\right)\cos\omega \qquad (A9b)$$

$$\frac{d\omega}{dt} = \frac{3nJ_{20}R_m^2}{a^2(1-e^2)^2}\left(1 - \frac{5}{4}\sin^2 i\right) + \frac{3nJ_{22}R_m^2}{a^2(1-e^2)^2}\left(1 - \frac{5}{2}\sin^2 i\right)\cos 2\Omega'$$

$$- \frac{3nJ_{30}R_m^3 \sin\omega}{8a^3(1-e^2)^3 e \sin i}\left[4e^2 - (35e^2+4)\sin^2 i + 5(7e^2+1)\sin^4 i\right] \qquad \text{(A9c)}$$

$$\frac{di}{dt} = -\frac{3nJ_{22}R_m^2 \sin i}{a^2(1-e^2)^2}\sin 2\Omega' + \frac{3nJ_{30}R_m^3 e \cos i}{2a^3(1-e^2)^3}\left(1 - \frac{5}{4}\sin^2 i\right)\cos\omega \qquad \text{(A9d)}$$

$$\frac{d\Omega}{dt} = -\frac{3nJ_{20}R_m^2 \cos i}{2a^2(1-e^2)^2} - \frac{3nJ_{22}R_m^2 \cos i}{a^2(1-e^2)^2}\cos 2\Omega'$$

$$+ \frac{3nJ_{30}R_m^3 e}{2a^3(1-e^2)^3}\cot i\left(1 - \frac{15}{4}\sin^2 i\right)\sin\omega \qquad \text{(A9e)}$$

From equation (A9) it is seen that $d\omega/dt$ and $d\Omega/dt$ have secular and long-period changes. All the rates of change of the elements except da/dt and de/dt have long-period changes (about 2 weeks) and all the rates of change of the elements except da/dt have a longer periodic change (period of the satellite orbit line of apsides). Some idea of the nature of the long-period change (long-period changes due to ω) in eccentricity and inclination can be obtained from equations (A9b) and (A9d). (In the long-period analysis it will be assumed that the effects which are periodic in Ω' have been averaged out.) If for the moment all quantities appearing in equations (A9b) and (A9d) are considered constant except the arguments of pericentron and if $d\omega/dt$ is approximated by its secular value, it is easy to integrate these expressions to obtain long-period changes in eccentricity and inclination. To account for this second long-period variation in eccentricity and inclination in the integration of equations (A9), the rates given by equations (A9) will be expanded in a Taylor's series about mean values (that is, over the period of rotation of the line of apsides) of inclination and eccentricity. If it is assumed that the values of e and i are not greatly different from the mean values, then only two terms of the expansion need be considered, that is, if $\frac{dE}{dt} = \dot{E}(a,e,i,\omega)$ represents any of the rates given in equations (A9), then $\dot{E}$ can be expanded about $\bar{e}$ and $\bar{i}$ to get the approximate or first-order relationship:

$$\dot{E}(a,e,i,\omega) = \dot{E}(a,\bar{e},\bar{i},\omega) + \left.\frac{\partial \dot{E}}{\partial e}\right|_{\bar{e},\bar{i}} \delta e + \left.\frac{\partial \dot{E}}{\partial i}\right|_{\bar{e},\bar{i}} \delta i \qquad \text{(A10)}$$

where

$$\left.\begin{aligned} \delta i &= i - \bar{i} \\ \delta e &= e - \bar{e} \end{aligned}\right\} \tag{A11}$$

and

$$\left.\begin{aligned} \bar{i} &= \frac{1}{2\pi}\int_0^{2\pi} i \, d\omega \\ \bar{e} &= \frac{1}{2\pi}\int_0^{2\pi} e \, d\omega \end{aligned}\right\} \tag{A12}$$

(Note, $\bar{a} = a$ since $\frac{da}{dt} = 0$.) Approximate expressions for δe and δi can be obtained by integration of de/dt and di/dt as given by equations (A9b) and (A9d) with the assumption that $d\omega/dt$ is approximately equal to only its secular value, that is, by the first term in equation (A9c) and that the values of e and i in these expressions are $\bar{e}$ and $\bar{i}$, respectively. Under these assumptions

$$\frac{de}{dt} \approx -\frac{3nR_m^3}{2a^3}\frac{J_{30}\sin\bar{i}}{\left(1-\bar{e}^2\right)^2}\left(1-\frac{5}{4}\sin^2\bar{i}\right)\cos\omega \tag{A13}$$

and

$$\frac{di}{dt} \approx \frac{3nJ_{30}R_m^3\bar{e}\cos\bar{i}}{2a^3\left(1-\bar{e}^2\right)^3}\left(1-\frac{5}{4}\sin^2\bar{i}\right)\cos\omega \tag{A14}$$

From this it may be seen that

$$\begin{aligned} e &\approx e_o - \frac{3nR_m^3}{2a^3\dot{\omega}_s}\frac{J_{30}\sin\bar{i}}{\left(1-\bar{e}^2\right)^2}\left(1-\frac{5}{4}\sin^2\bar{i}\right)\int_{\omega_o}^{\omega}\cos\omega\,d\omega \\ &= e_o - \frac{J_{30}}{2J_{20}}\frac{R_m}{a}\sin\bar{i}(\sin\omega - \sin\omega_o) \end{aligned} \tag{A15}$$

and

$$i \approx i_o + \frac{3nJ_{30}R_m^3\bar{e}\cos\bar{i}}{2a^3(1-\bar{e}^2)^3\dot{\omega}_s}\left(1-\frac{5}{4}\sin^2\bar{i}\right)\int_{\omega_o}^{\omega}\cos\omega\,d\omega$$

$$= i_o + \frac{J_{30}R_m\bar{e}\cos\bar{i}}{2J_{20}a(1-\bar{e}^2)}(\sin\omega - \sin\omega_o) \qquad \text{(A16)}$$

Substitution of equations (A15) and (A16) into equation (A12) gives for $\bar{e}$ and $\bar{i}$ the following approximations:

$$\left.\begin{aligned}\bar{e} &= e_o + \frac{J_{30}}{2J_{20}}\frac{R_m}{a}\sin\bar{i}\sin\omega_o \\ \bar{i} &= i_o - \frac{J_{30}}{2J_{20}}\frac{R_m\bar{e}\cos\bar{i}}{a(1-\bar{e}^2)}\sin\omega_o\end{aligned}\right\} \qquad \text{(A17)}$$

Then

$$\delta e = e - \bar{e} = -\frac{J_{30}}{2J_{20}}\frac{R_m}{a}\sin\bar{i}\sin\omega \qquad \text{(A18)}$$

$$\delta i = i - \bar{i} = \frac{J_{30}}{2J_{20}}\frac{R_m\bar{e}\cos\bar{i}}{a(1-\bar{e}^2)}\sin\omega \qquad \text{(A19)}$$

These values can be substituted into equation (A10) to obtain an approximate value of $\dot{E}$ in terms of mean values of eccentricity and inclination. The partial derivatives to be used in equation (A10) are listed as follows (again, it is assumed that all effects which are periodic in Ω' have been averaged out):

$$\left.\frac{\partial\dot{\omega}}{\partial e}\right|_{\bar{e},\bar{i}} = \frac{12nJ_{20}R_m^2\bar{e}}{a^2(1-\bar{e}^2)^3}\left(1-\frac{5}{4}\sin^2\bar{i}\right) + O(J_{30}) \qquad \text{(A20a)}$$

$$\left.\frac{\partial\dot{\Omega}}{\partial e}\right|_{\bar{e},\bar{i}} = -\frac{6nJ_{20}R_m^2\bar{e}}{a^2(1-\bar{e}^2)^3}\cos\bar{i} + O(J_{30}) \qquad \text{(A20b)}$$

$$\left.\frac{\partial\dot{\omega}}{\partial e}\right|_{\bar{e},\bar{i}} = -\frac{15nJ_{20}R_m^2}{2a^2(1-\bar{e}^2)^2}\sin\bar{i}\cos\bar{i} + O(J_{30}) \qquad \text{(A20c)}$$

$$\left.\frac{\partial\dot{a}}{\partial e}\right|_{\bar{e},\bar{i}} = 0 \qquad \text{(A20d)}$$

$$\left.\frac{\partial \dot{e}}{\partial e}\right|_{\bar{e},\bar{i}} = O(J_{30}) \tag{A20e}$$

$$\left.\frac{\partial\left(\frac{di}{dt}\right)}{\partial e}\right|_{\bar{e},\bar{i}} = O(J_{30}) \tag{A20f}$$

Quantities of the order of J_{30} in the preceding equations were not evaluated since, as is shown later, such terms contribute terms of the order of J_{30}^2/J_{20}. These terms are considered second order with respect to terms of the order of J_{30}.

Substitution of the results from equations (A20) into equation (A10) gives the following secular and long-period rates:

$$\frac{d\omega}{dt} = \frac{3nJ_{20}R_m^2}{a^2(1-\bar{e}^2)^2}\left(1 - \frac{5}{4}\sin^2\bar{i}\right) + \frac{3nJ_{30}R_m^3}{2a^3(1-\bar{e}^2)^3}\,\frac{\sin^2\bar{i} - \bar{e}^2\cos^2\bar{i}}{e\sin\bar{i}}\left(1 - \frac{5}{4}\sin^2\bar{i}\right)\sin\omega + O\left(\frac{J_{30}^2}{J_{20}}\right) \tag{A21a}$$

$$\frac{d\Omega}{dt} = -\frac{3nJ_{20}R_m^2\cos\bar{i}}{2a^2(1-\bar{e}^2)^2} + \frac{3nJ_{30}R_m^3\bar{e}\cos\bar{i}\left(1 - \frac{5}{4}\sin^2\bar{i}\right)}{2a^3(1-\bar{e}^2)^3\sin\bar{i}}\sin\omega + O\left(\frac{J_{30}^2}{J_{20}}\right) \tag{A21b}$$

$$\frac{di}{dt} = \frac{3nJ_{30}R_m^3\cos\bar{i}}{2a^3(1-\bar{e}^2)^3}\left(1 - \frac{5}{4}\sin^2\bar{i}\right)\cos\omega + O\left(\frac{J_{30}^2}{J_{20}}\right) \tag{A21c}$$

$$\frac{de}{dt} = -\frac{3nR_m^3}{2a^3}\,\frac{J_{30}\sin\bar{i}}{(1-\bar{e}^2)^2}\left(1 - \frac{5}{4}\sin^2\bar{i}\right)\cos\omega + O\left(\frac{J_{30}^2}{J_{20}}\right) \tag{A21d}$$

$$\frac{da}{dt} = 0 \tag{A21e}$$

The change in the elements which are periodic in Ω' can be obtained by considering the terms in equations (A9), which contain Ω'. These equations can be put into an approximate equivalent form that can be integrated by replacing the value of i in the coefficients by its mean value taken over the period of the moon's rotation about its polar axis. Neither e nor a need be considered as mean values since they do not have a change which is periodic in Ω'.

APPENDIX A

If the total rates of change in the elements (excluding short-period effects) as given by equations (A9) are separated into terms denoted by a subscript 2, 3, or 4 according to whether they are periodic in Ω', periodic in ω, or secular, they can be written in terms of the mean elements as follows:

$$\left(\frac{da}{dt}\right)_2 = \left(\frac{da}{dt}\right)_3 = \left(\frac{da}{dt}\right)_4 = 0 \tag{A22}$$

$$\left(\frac{de}{dt}\right)_2 = 0 \tag{A23a}$$

$$\left(\frac{de}{dt}\right)_3 = -\frac{3nR_m^3}{2a^3}\frac{J_{30}\sin\bar{i}}{(1-\bar{e}^2)^2}\left(1-\frac{5}{4}\sin^2\bar{i}\right)\cos\omega \tag{A23b}$$

$$\left(\frac{de}{dt}\right)_4 = 0 \tag{A23c}$$

$$\left(\frac{di}{dt}\right)_2 = -\frac{3nJ_{22}R_m^2\sin\bar{i}}{a^2(1-e^2)^2}\sin 2\Omega' \tag{A24a}$$

$$\left(\frac{di}{dt}\right)_3 = \frac{3nJ_{30}R_m^3\cos\bar{i}}{2a^3(1-\bar{e}^2)^3}\left(1-\frac{5}{4}\sin^2\bar{i}\right)\cos\omega \tag{A24b}$$

$$\left(\frac{di}{dt}\right)_4 = 0 \tag{A24c}$$

$$\left(\frac{d\omega}{dt}\right)_2 = \frac{3nJ_{22}R_m^2}{a^2(1-e^2)^2}\left(1-\frac{5}{2}\sin^2\bar{i}\right)\cos 2\Omega' \tag{A25a}$$

$$\left(\frac{d\omega}{dt}\right)_3 = \frac{3nJ_{30}R_m^3}{2a^3(1-\bar{e}^2)^3}\frac{\sin^2\bar{i}-\bar{e}^2\cos^2\bar{i}}{\bar{e}\sin\bar{i}}\left(1-\frac{5}{4}\sin^2\bar{i}\right)\sin\omega \tag{A25b}$$

$$\left(\frac{d\omega}{dt}\right)_4 = \frac{3nJ_{20}R_m^2}{a^2(1-\bar{e}^2)^2}\left(1-\frac{5}{4}\sin^2\bar{i}\right) \tag{A25c}$$

$$\left(\frac{d\Omega}{dt}\right)_2 = -\frac{3nJ_{22}R_m^2 \cos \bar{i}}{a^2(1 - e^2)^2} \cos 2\Omega' \tag{A26a}$$

$$\left(\frac{d\Omega}{dt}\right)_3 = \frac{3nJ_{30}R_m^3\bar{e}}{2a^3(1 - \bar{e}^2)^3} \frac{\cos \bar{i}}{\sin \bar{i}}\left(1 - \frac{5}{4} \sin^2\bar{i}\right)\sin \omega \tag{A26b}$$

$$\left(\frac{d\Omega}{dt}\right)_4 = -\frac{3nJ_{20}R_m^2 \cos \bar{i}}{2a^2(1 - \bar{e}^2)^2} \tag{A26c}$$

The secular changes can be obtained from equations (A22), (A23c), (A24c), (A25c), and (A26c) as

$$(\Delta a)_4 = (\Delta e)_4 = (\Delta i)_4 = 0 \tag{A27a}$$

$$(\Delta\omega)_4 = \frac{3nJ_{20}R_m^2}{a^2(1 - \bar{e}^2)^2}\left(1 - \frac{5}{4} \sin^2\bar{i}\right)t \tag{A27b}$$

$$(\Delta\Omega)_4 = -\frac{3nJ_{20}R_m^2 \cos \bar{i}}{2a^2(1 - \bar{e}^2)^2} t \tag{A27c}$$

The rates periodic in Ω' can be integrated by use of the approximate expression

$$\frac{d\Omega'}{dt} = n_1 \tag{A28}$$

(where n_1 is the rate of rotation of the moon about its polar axis) to get

$$(\Delta i)_2 = \frac{3nJ_{22}R_m^2 \sin \bar{i}}{2a^2(1 - \bar{e}^2)^2 n_1}\left(\cos 2\Omega' - \cos 2\Omega_o'\right) \tag{A29a}$$

$$(\Delta\omega)_2 = \frac{3nJ_{22}R_m^2}{2a^2(1 - e^2)^2 n_1}\left(1 - \frac{5}{4} \sin^2\bar{i}\right)\left(\sin 2\Omega' - \sin 2\Omega_o'\right) \tag{A29b}$$

$$(\Delta\Omega)_2 = -\frac{3nJ_{22}R_m^2 \cos \bar{i}}{2a^2(1 - e^2)n_1}\left(\sin 2\Omega' - \sin 2\Omega_o'\right) \tag{A29c}$$

APPENDIX A

The rates periodic in ω can be integrated by assuming that the major rate of change of ω is due to its secular rate

$$\frac{d\omega}{dt} \approx \left(\frac{d\omega}{dt}\right)_4 = \frac{3nJ_{20}R_m^2}{a^2(1 - \bar{e}^2)^2}\left(1 - \frac{5}{4}\sin^2\bar{i}\right) \tag{A30}$$

This gives

$$(\Delta e)_3 = -\frac{J_{30}R_m \sin \bar{i}}{2aJ_{20}}(\sin \omega - \sin \omega_0) \tag{A31a}$$

$$(\Delta i)_3 = \frac{J_{30}R_m\bar{e} \cos \bar{i}}{2aJ_{20}(1 - \bar{e}^2)}(\sin \omega - \sin \omega_0) \tag{A31b}$$

$$(\Delta \omega)_3 = -\frac{J_{30}R_m}{2aJ_{20}(1 - \bar{e}^2)} \frac{\sin^2\bar{i} - \bar{e}^2\cos^2\bar{i}}{\bar{e} \sin \bar{i}}(\cos \omega - \cos \omega_0) \tag{A31c}$$

$$(\Delta \Omega)_3 = -\frac{J_{30}R_m\bar{e}}{2aJ_{20}(1 - \bar{e}^2)} \cot \bar{i}(\cos \omega - \cos \omega_0) \tag{A31d}$$

To obtain a comparison of the relative magnitude of these changes, the maximum amplitudes of the rates for a given orbit are given in the following chart:

Element \ Subscript	2	3	4
de/dt, per day	0	0.00125	0
di/dt, deg/day	0.048	0.195	0
dω/dt, deg/day	0.090	0.278	1.142
dΩ/dt, deg/day	0.124	0.103	0.635

For computation, the following orbital elements are considered:

$$\bar{a} = 2224 \text{ kilometers}$$

$$\bar{e} = 0.1972$$

$$\bar{i} = 21^\circ$$

with

$$J_{20} = 2.073 \times 10^{-4}$$

$$J_{22} = -2.03 \times 10^{-5}$$

$$J_{30} = -9.3 \times 10^{-5}$$

APPENDIX B

SECOND-ORDER ANALYSIS

The following analysis is second order in the sense that an approximate expression which includes both secular and long-period (periodic in ω) effects are used in the expression for $d\omega/dt$. This expression for $d\omega/dt$ is then used in the determination of Δr_p rather than the approximate expression $\left(\frac{d\omega}{dt}\right)_4$. According to equations (A25b) and (A25c), the sum of the secular and second long-period change in the argument of pericentron is

$$\frac{d\omega}{dt} = \frac{3nJ_{20}R_m^2}{a^2(1 - \bar{e}^2)^2}\left(1 - \frac{5}{4}\sin^2\bar{i}\right)\left[1 + \frac{J_{30}R_m \sin\omega}{2J_{20}a(1 - \bar{e}^2)}\frac{\sin^2\bar{i} - \bar{e}^2\cos^2\bar{i}}{\bar{e}\sin\bar{i}}\right] \tag{B1}$$

For convenience, the following definitions are presented:

$$\dot{\omega}_s = \frac{3nJ_{20}R_m^2}{a^2(1 - \bar{e}^2)^2}\left(1 - \frac{5}{4}\sin^2\bar{i}\right) \tag{B2}$$

$$f = \frac{J_{30}R_m}{2J_{20}a(1 - \bar{e}^2)}\frac{\sin^2\bar{i} - \bar{e}^2\cos^2\bar{i}}{\bar{e}\sin\bar{i}} \tag{B3}$$

Substituting equations (B2) and (B3) into equation (B1) gives

$$\frac{d\omega}{dt} = \dot{\omega}_s(1 + f\sin\omega) \tag{B4}$$

Integration of equation (B4) yields

$$t = \frac{1}{\dot{\omega}_s}\int_{\omega_o}^{\omega}\frac{d\omega}{1 + f\sin\omega} \tag{B5}$$

and relates t and ω by the relation

$$t = \frac{2}{\dot{\omega}_s\sqrt{1 - f^2}}\left[\pi\delta + \tan^{-1}\left(\frac{f + \tan\frac{\omega}{2}}{\sqrt{1 - f^2}}\right) - \tan^{-1}\left(\frac{f + \tan\frac{\omega_o}{2}}{\sqrt{1 - f^2}}\right)\right] \tag{B6}$$

where $\delta = 1$ when $\omega_o < \pi < \omega$ and $\delta = 0$ for all other values of ω and ω_o. In all cases $\omega_o \leq \omega < \omega_o + 2\pi$.

To the second order in f, equation (B6) can be expanded to obtain

$$t = \frac{1}{\dot{\omega}_s}\left\{\omega - \omega_o + f(\cos\omega - \cos\omega_o) + \frac{f^2}{2}\left[(\omega - \omega_o) - \frac{1}{2}(\sin 2\omega - \sin 2\omega_o)\right] + O(f^3)\right\} \tag{B7}$$

Equation (B7) is accurate only when f is small compared with unity. Since the long-period change in the pericentron altitude is given as

$$\Delta r_p = -a\,\Delta e \tag{B8}$$

an expression is needed for the long-period change in eccentricity. This expression is obtained from the rate de/dt given in equation (A21d) which can be written as

$$\frac{de}{dt} = -\frac{J_{30}R_m \sin\bar{i}}{2aJ_{20}}\dot{\omega}_s \cos\omega \tag{B9}$$

Substitution of $d\omega/dt$ from equation (B4) into equation (B9) gives

$$\Delta e = -\frac{J_{30}R_m \sin\bar{i}}{2aJ_{20}}\int_{\omega_o}^{\omega}\frac{\cos\omega}{1 + f\sin\omega}\,d\omega$$

$$= -\frac{J_{30}R_m \sin\bar{i}}{2J_{20}af}\log\left(\frac{1 + f\sin\omega}{1 + f\sin\omega_o}\right) \tag{B10}$$

which gives the following long-period change in the pericentron altitude

$$\Delta r_p = \frac{J_{30}R_m \sin\bar{i}}{2fJ_{20}}\log\left(\frac{1 + f\sin\omega}{1 + f\sin\omega_o}\right) \tag{B11}$$

It may be seen that equation (B11) reduces to the first-order result for Δr_p whenever f is small. This condition is illustrated by the expansion of equation (B11) in a Taylor's series, which is

APPENDIX B

$$\Delta r_p = \frac{J_{30} R_m \sin \bar{i}}{2 J_{20} f} \left[f \sin \omega - \frac{1}{2} f^2 \sin^2 \omega + \frac{1}{3} f^3 \sin^3 \omega \right.$$

$$\left. - f \sin \omega_o + \frac{1}{2} f^2 \sin^2 \omega_o - \frac{1}{3} f^3 \sin^3 \omega_o + O\left(f^4\right) \right]$$

$$\Delta r_p = \frac{J_{30} R_m \sin \bar{i}}{2 J_{20}} (\sin \omega - \sin \omega_o) \left[1 - \frac{f}{2} (\sin \omega + \sin \omega_o) \right.$$

$$\left. + \frac{f^2}{3} \left(\sin^2 \omega + \sin \omega \sin \omega_o + \sin^2 \omega_o \right) + O\left(f^3\right) \right] \qquad \text{(B12)}$$

Caution should be used in the application of equation (B12) since it is restricted to small values of f.

APPENDIX C

TIME HISTORY OF PERICENTRON LOCATION AND SOLAR POSITION

The dependence of latitude and longitude of pericentron, solar positions, and values of argument of pericentron on inclination can be obtained from the following sketch:

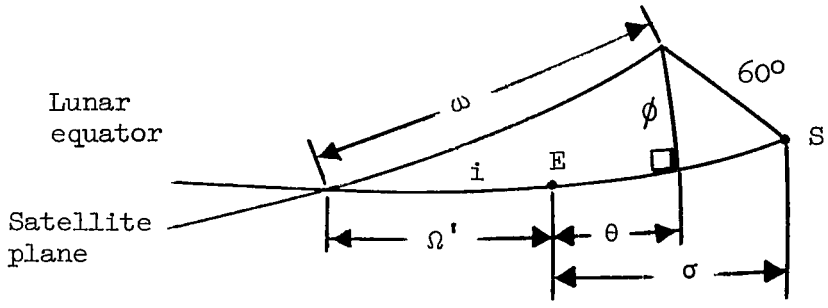

Application of spherical trigonometry to the sketch results in the following relations:

$$\left.\begin{aligned} \sin\phi &= \sin i \sin\omega \\ \cos\theta\cos\phi &= -\sin\Omega'\sin\omega\cos i + \cos\Omega'\cos\omega \\ \sin\theta\cos\phi &= \cos\Omega'\sin\omega\cos i + \sin\Omega'\cos\omega \\ \cos(\sigma-\theta)\cos\phi &= \tfrac{1}{2} \end{aligned}\right\} \qquad (C1)$$

Given initial values of ω and Ω', the initial latitude and longitude of the argument of pericentron as a function of i can be found from equation (C1) as

$$\left.\begin{aligned} \sin\phi_o &= \sin i \sin\omega_o \\ \cos\theta_o &= -\frac{\sin\Omega_o'\sin\omega_o\cos i + \cos\Omega_o'\cos\omega_o}{\sqrt{1-\sin^2 i\sin^2\omega_o}} \\ \sin\theta_o &= \frac{\cos\Omega_o'\sin\omega_o\cos i + \sin\Omega_o'\cos\omega_o}{\sqrt{1-\sin^2 i\sin^2\omega_o}} \end{aligned}\right\} \qquad (C2)$$

The initial values of the solar positions for the initial longitude and latitude can be obtained from the expression

$$\cos(\sigma_o - \theta_o) = \frac{1}{2\sqrt{1 - \sin^2 i \sin^2 \omega_o}} \tag{C3}$$

The subsequent change in ϕ with time is obtained by substituting the following first-order expressions for ω into equation (C1):

$$\omega = \omega_o + \frac{3nJ_{20}R_m^2}{a^2(1 - e^2)^2}\left(1 - \frac{5}{4}\sin^2 i\right)t \tag{C4}$$

The change of θ with time is obtained as

$$\theta = \theta_o - (13.2 - \dot{\Omega})t = \theta_o - \left[13.2 + \frac{3nJ_{20}R_m^2 \cos i}{2a^2(1 - e^2)^2}\right]t \tag{C5}$$

The change in solar position σ, with time is obtained by substituting into the last equation in equation (C1) the time-dependent values of ϕ and θ just described.

REFERENCES

1. Kaula, William M.: The Investigation of the Gravitational Fields of the Moon and Planets With Artificial Satellites. Vol. 5 of Advances in Space Science and Technology, Frederick I. Ordway, III, ed., Academic Press, Inc., 1963, pp. 210-230.

2. Byerly, William Elwood: An Elementary Treatise on Fourier's Series and Spherical Cylindrical, and Ellipsoidal Harmonics, With Applications to Problems in Mathematical Physics. Ginn and Co., 1893.

3. Brouwer, Dirk; and Clemence, Gerald M.: Methods of Celestial Mechanics. Academic Press, Inc., 1961.

4. Kozai, Yoshihide: The Motion of a Close Earth Satellite. Astron. J., vol. 64, no. 9, Nov. 1959, pp. 367-377.

5. Tisserand, François Félix: Traité de Mécanique Céleste. Vol. 1, Gauthier-Villars et Fils (Paris), 1889.

6. Moulton, Forest Ray: An Introduction to Celestial Mechanics. Second rev. ed., New York: The Macmillan Co., c.1914.

2/22/85

"The aeronautical and space activities of the United States shall be conducted so as to contribute . . . to the expansion of human knowledge of phenomena in the atmosphere and space. The Administration shall provide for the widest practicable and appropriate dissemination of information concerning its activities and the results thereof."

—NATIONAL AERONAUTICS AND SPACE ACT OF 1958

NASA SCIENTIFIC AND TECHNICAL PUBLICATIONS

TECHNICAL REPORTS: Scientific and technical information considered important, complete, and a lasting contribution to existing knowledge.

TECHNICAL NOTES: Information less broad in scope but nevertheless of importance as a contribution to existing knowledge.

TECHNICAL MEMORANDUMS: Information receiving limited distribution because of preliminary data, security classification, or other reasons.

CONTRACTOR REPORTS: Technical information generated in connection with a NASA contract or grant and released under NASA auspices.

TECHNICAL TRANSLATIONS: Information published in a foreign language considered to merit NASA distribution in English.

TECHNICAL REPRINTS: Information derived from NASA activities and initially published in the form of journal articles.

SPECIAL PUBLICATIONS: Information derived from or of value to NASA activities but not necessarily reporting the results of individual NASA-programmed scientific efforts. Publications include conference proceedings, monographs, data compilations, handbooks, sourcebooks, and special bibliographies.

Details on the availability of these publications may be obtained from:

SCIENTIFIC AND TECHNICAL INFORMATION DIVISION

NATIONAL AERONAUTICS AND SPACE ADMINISTRATION

Washington, D.C. 20546